



Article

Thioether-Linked Liquid Crystal Trimers: Odd–Even Effects of Spacers and the Influence of Thioether Bonds on Phase Behavior

Yuki Arakawa , Kenta Komatsu, Yuko Ishida, Takuma Shiba and Hideto Tsuji 

Department of Applied Chemistry and Life Science, Graduate School of Engineering, Toyohashi University of Technology, 1-1 Hibarigaoka, Tempaku-cho, Toyohashi 441-8580, Japan; komatsu.kenta.qr@tut.jp (K.K.); ishida.yuko.rm@tut.jp (Y.I.); shiba.takuma.wt@tut.jp (T.S.); ht003@edu.tut.ac.jp (H.T.)

* Correspondence: arakawa@tut.jp

Abstract: We report the synthesis, phase-transition behavior, and mesophase structures of the first homologous series of thioether-linked liquid crystal (LC) trimers, 4,4'-bis[ω -(4-cyanobiphenyl-4'-ylthio)alkoxy]biphenyls (CBS n OBO n SCB with a wide range of spacer carbon numbers, $n = 3$ –11). All CBS n OBO n SCB homologs exhibited LC phases. Interestingly, even- n and odd- n homologs showed monotropic layered smectic A (SmA) and pseudo-layered twist-bend nematic (N_{TB}) phases, respectively, below a nematic (N) phase. This alternate formation, which depends on spacer chain parity, is attributed to different average molecular shapes, which are associated with the relative orientations of the biphenyl moieties: linear and bent shapes for even- n and odd- n homologs, respectively. In addition, X-ray diffraction analysis indicated a strong cybotactic N phase tendency, with a triply intercalated structure. The phase-transition behavior and LC phase structures of thioether-linked CBS n OBO n SCB were compared with those of the all-ether-linked classic LC trimers CBO n OBO n OCB. Overall, thioether linkages endowed CBS n OBO n SCB with a monotropic LC tendency and lowered phase-transition temperatures, compared to those of CBO n OBO n OCB, for the same n . This is attributed to enhanced flexibility and bending (less molecular anisotropy) of the molecules, caused by the greater bond flexibility and smaller inner bond angles of the C–S–C bonds, compared to those of the C–O–C bonds.

Keywords: liquid crystal trimer; odd-even effect; thioether; twist-bend nematic phase; smectic phase



Citation: Arakawa, Y.; Komatsu, K.; Ishida, Y.; Shiba, T.; Tsuji, H. Thioether-Linked Liquid Crystal Trimers: Odd–Even Effects of Spacers and the Influence of Thioether Bonds on Phase Behavior. *Materials* **2022**, *15*, 1709. <https://doi.org/10.3390/ma15051709>

Academic Editor: Richard J. Mandle

Received: 31 January 2022

Accepted: 20 February 2022

Published: 24 February 2022

Publisher's Note: MDPI stays neutral with regard to jurisdictional claims in published maps and institutional affiliations.



Copyright: © 2022 by the authors. Licensee MDPI, Basel, Switzerland. This article is an open access article distributed under the terms and conditions of the Creative Commons Attribution (CC BY) license (<https://creativecommons.org/licenses/by/4.0/>).

1. Introduction

Liquid crystal (LC) dimers, trimers, and higher oligomers have been widely investigated [1]. They consist of more than two rigid mesogenic groups linked linearly via flexible alkylene spacers, as shown in Figure 1. A fascinating feature of LC oligomers is the odd–even effect of the number of spacer-atoms on various LC properties, associated with the relative orientation of rigid mesogenic groups, or different molecular geometries. In simple dimers, even-number spacers roughly direct the mesogenic groups to a parallel alignment, forming a relatively straightened stretched Z-like shape, whereas odd-number spacers form bent shapes, as shown in Figure 1. This contrast generates odd–even oscillations in various physical properties associated with the orientational order parameter [1–6].

The average geometrical differences influence the types of LC phases induced [7,8]. The discovery of a heliconical twist-bend nematic (N_{TB}) phase for bent LC dimers with odd-number spacers has provided a strong impetus to explore oligomeric LC materials in the last decade [9–12]. The N_{TB} phase has nanoscopic heliconical structures with pitches ranging from several nanometers to tens of nanometers [13–15]. Interestingly, chiral helical structures develop from achiral bent molecules, with the degeneracy of right- and left-handed helical structures. These helical structures cause the N_{TB} phase to apparently involve layered smectic (Sm) phase-like behavior, which is pseudo-layered in nature [16–20].

Physical properties of twist-bend nematogens have been extensively studied for basic scientific reasons as well as potential applications [21–32]. However, the phase identification and nanoscopic structures of the N_{TB} phase require further investigation [33–35].

Intensive studies have confirmed that many LC dimers [36–49] and some oligomers [50–54], polymers [55], and bent-core molecules [56,57] exhibit the N_{TB} phase. Higher oligomers that have more mesogenic units are less likely to form an N_{TB} phase [55]. In contrast to the many reports on dimer homologs containing the same mesogenic cores and different alkylene spacers, only one homologous series of LC trimers has been studied as twist-bend nematogenic higher oligomer homologs [58]. This is a homologous series of the all-ether-linked biphenyl-based LC trimers, 4,4'-bis[ω -(4-cyanobiphenyl-4'-yloxy)alkoxy]biphenyls (CBO n OBO n OCB with spacer carbon numbers, $n = 4$ –11, where B, CB, and O denote central 4,4'-linked biphenyl, bilateral cyanobiphenyl groups, and ether linkages, respectively), which are the classic LC trimer homologs [59–61]. It has been reported that the CBO n OBO n OCB homologs alternately form layered smectic A (SmA) and pseudo-layered N_{TB} phases for even- n and odd- n , respectively [58]. Furthermore, their outer thioether-linked analogs, CBS n OBO n SCB with odd $n = 7$ and 9 (Figure 2a) also exhibit the N_{TB} phase below the N phase [62,63]. Flexible C–S–C bonds have smaller bond angles ($\sim 103^\circ$) than ethers (C–O–C; $\sim 118^\circ$). This generally reduces the ability of calamitic molecules to form LCs, by providing greater conformational and steric bulkiness [62–67]. In contrast, the smaller bond angle of the flexible C–S–C bond synergistically contributes to N_{TB} phase induction and stabilization [62,63,68–74] by enhancing the bent shape and flexibility of LC oligomers with odd- n spacers, as shown in Figure 1. This is also the case for the higher chalcogen selenoether C–Se–C bond [75]. To date, other CBS n OBO n SCB homologs including even- n have not been synthesized, so the influences of thioether linkages on the phase-transition behavior, its odd–even effects, and LC phase structures of a homologous series of LC trimers have not been studied.

In this context, we developed a homologous series of the thioether-linked CBS n OBO n SCB trimers possessing a wide variety of odd and even numbers of carbon atoms in the alkylene spacers ($n = 3$ –11), of which $n = 7$ and 9 have been previously reported [62,63]. Their phase transitions and structures were investigated by polarized optical microscopy (POM), differential scanning calorimetry (DSC), and X-ray diffractometry (XRD), and compared with those of the corresponding all-ether-linked trimers, CBO n OBO n OCB [58].

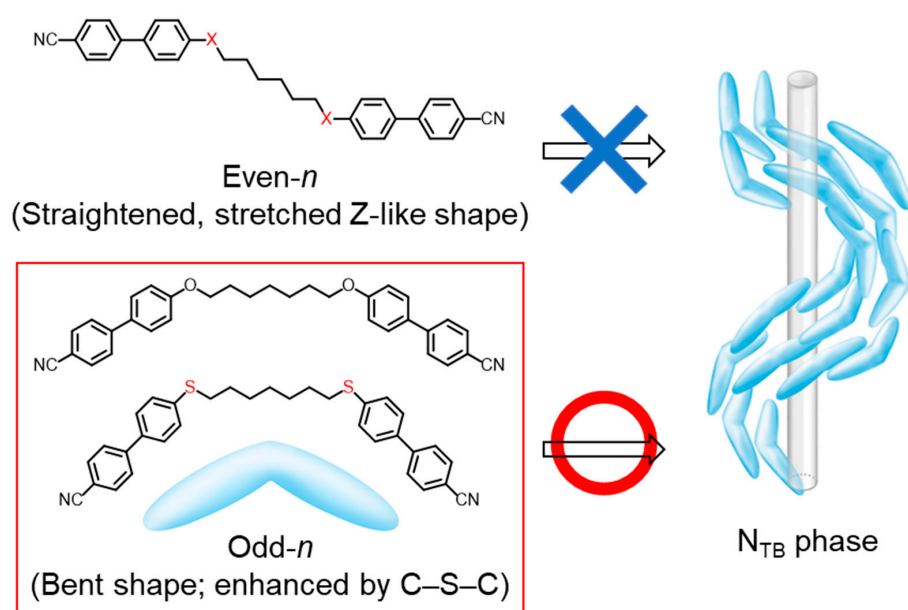


Figure 1. Molecular geometries (shapes) imposed by spacer parity of semi-flexible spacers, and schematic model of the N_{TB} phase formed by bent molecules. The model of the N_{TB} phase was reproduced from ref. [70] with permission from Wiley.

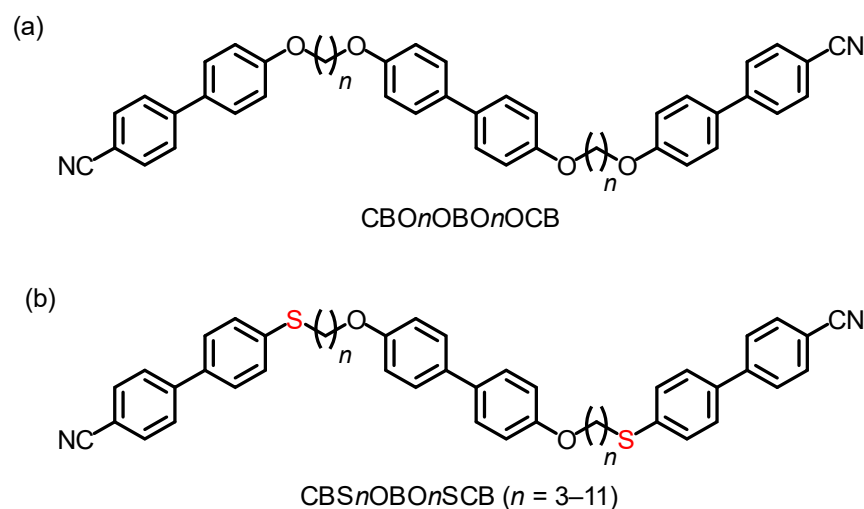


Figure 2. Molecular structures of (a) all-ether-linked biphenyl-based 4,4'-bis[ω -(4-cyanobiphenyl-4'-yloxy)alkoxy]biphenyl homologs ($\text{CBO}_n\text{OBO}_n\text{OCB}$, $n = 4-11$) (previously reported) [58–61], and (b) their outer thioether-linked homologs ($\text{CBS}_n\text{OBO}_n\text{SCB}$, $n = 3-11$) (the present study), in which $n = 7$ and 9 have been previously reported [62,63].

2. Materials and Methods

Synthetic schemes and procedures for $\text{CBS}_n\text{OBO}_n\text{SCB}$ are described in the Supplementary Material. Molecular structures were determined by ^1H and ^{13}C nuclear magnetic resonance (NMR) spectroscopy, using a JNM-ECX500 (500 MHz for ^1H , and 125 MHz for ^{13}C NMR) or a JNM-ESC400 (400 MHz for ^1H , and 100 MHz for ^{13}C NMR) instrument (JEOL, Ltd., Tokyo, Japan). ^1H and ^{13}C NMR data are provided in the Supplementary Material, excluding ^{13}C NMR data of even- n homologs. Their spectra could not be obtained because they had poor solubility similar to ether-linked $\text{CBO}_n\text{OBO}_n\text{OCB}$ trimers [58]. Phase identification was determined by POM using an Olympus polarizing microscope (BX50, Tokyo, Japan), equipped with a Linkam temperature controller (LK-600PM, Surrey, UK). POM observations were carried out for the samples that were placed between non-treated thin glass cells. The obtained POM microphotographs are shown in the main text and Supplementary Material. Phase-transition temperatures for crystal (Cr)–N or Cr–isotropic (I) phase transitions upon heating (melting point: T_m), crystallization upon cooling (T_{Cr}), N–I phase transitions upon heating and cooling (T_{NI} and T_{IN} , respectively), monotropic N–SmA and N– N_{NTB} phase transitions upon cooling (T_{NS} and T_{NNTB} , respectively), and associated entropy changes (ΔS) scaled by the gas constant (R) on T_m , T_{Cr} , T_{NI} , and T_{IN} ($\Delta S_m/R$, $\Delta S_{Cr}/R$, $\Delta S_{NI}/R$, and $\Delta S_{IN}/R$, respectively), were determined by DSC, using a DSC-60 Plus instrument (Shimadzu, Kyoto, Japan), which was calibrated using indium. DSC measurements were conducted upon heating-to-cooling-to-heating cycles at a rate of $10\text{ }^\circ\text{C min}^{-1}$ under a flow of nitrogen gas. Samples (3–4 mg) weighed accurately in aluminum pans were used for the DSC measurements. The obtained DSC curves are shown in the Supplementary Material, except for those of the previously reported $\text{CBS}_n\text{OBO}_n\text{SCB}$ ($n = 7$ and 9) [62,63]. In addition, the phase-transition temperatures for the elusive monotropic LC phases were determined by POM. The N phases of $\text{CBS}_9\text{OBO}_9\text{SCB}$ and $\text{CBO}_9\text{OBO}_9\text{OCB}$ were analyzed by XRD measurements, using a D8 DISCOVER diffractometer, with a Cu $K\alpha$ radiation source, equipped with a Vantec-500 detector (Bruker, Billerica, MA, USA). Capillary glass tubes with 1.5 mm diameter (WJM-Glass Müller GmbH, Berlin, Germany), in which the material was kept, were sandwiched between permanent magnets in a homemade folder. Measurements were carried out at different temperatures upon cooling from each I phase, to remove the thermal history of the materials.

3. Results and Discussion

3.1. Phase-Transition Behavior of CBS n OBO n SCB

The phase-transition results obtained upon first heating and cooling CBS n OBO n SCB are listed in Table 1. The different T_m and phase transitions, which could be associated with the existence of crystal polymorphs, were observed depending on the thermal courses and conditions. For simplicity, these are not discussed in this paper. All CBS n OBO n SCB trimers exhibited the conventional N phases. More specifically, the N phases of $n = 4, 7-9,$ and 11 were enantiotropic, while those of $n = 3, 5, 6,$ and 10 were monotropic. Notably, even- n and odd- n CBS n OBO n SCB trimers (for $n = 5-11$) exhibited monotropic layered Sm and pseudo-layered N_{TB} phases, respectively, below the N phase temperature, as reported for the all-ether-linked CBO n OBO n OCB trimers [58]. This is a part of the odd–even effect on the phase-transition behavior of LC trimers. Considering that the N_{TB} phase is induced only by bent molecules, this alternate formation of Sm and N_{TB} phases could be ascribed to the dependence of the average molecular shapes on the parity of n for the LC trimer (straightened and bent shapes for even- n and odd- n homologs, respectively). Even- n homologs ($n = 6, 8,$ and 10) exhibited fan-shaped textures of layered Sm phases. These Sm textures were observed in the supercooled N phase domains or droplets after crystallization of major parts, as shown in Figures 3a,b, S4 and S5, for $n = 6, 8,$ and 10, respectively. Therefore, these monotropic Sm phases were unsuitable for further characterization using XRD. Considering the homeotropic dark textures reported for the Sm phases of all-ether-linked CBO n OBO n OCB homologs with even- n [58,61], those of thioether-linked CBS n OBO n SCB could be characterized as orthogonal SmA phases. POM microphotographs of the N_{TB} phase of CBS11OBO11SCB are shown in Figure 3c,d, where blocky and focal conic-like textures were observed in a non-treated glass cell. These textures are characteristic of the N_{TB} phase, and are caused by the undulations of the pseudo-periodic layers of the helical structures [14,17,19]. The N–N_{TB} phase transitions for CBS5OBO5SCB were observed in small, supercooled N domains and droplets by POM (Figure S3). The results for $n = 7$ and 9 have been previously reported [62,63]. In this study, however, the above-mentioned optical textural changes, which indicate the presence of monotropic SmA or N_{TB} phases, were not observed for the shortest even/odd CBS n OBO n SCB homologs ($n = 3$ and 4), which exhibited only the N phase, as shown in Figures S1 and S2.

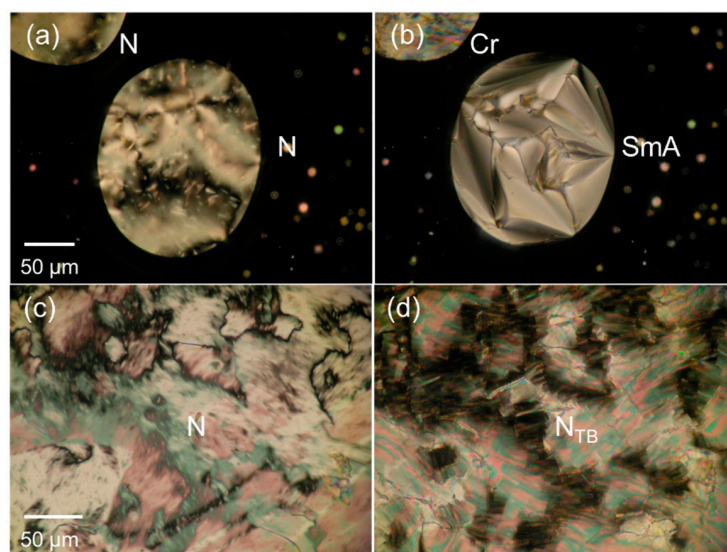


Figure 3. POM images of CBS6OBO6SCB [(a,b)] and CBS11OBO11SCB [(c,d)]: (a) Marble and schlieren textures (N phase) at 210 °C; (b) Fan-shaped and focal conic textures (SmA phase) with a Cr region at 178 °C; (c) Marble and schlieren textures (N phase) at 130 °C; (d) Blocky texture (N_{TB} phase) at 119 °C in a non-treated glass cell.

Table 1. Thermal phase sequences, phase-transition temperatures, and associated entropy changes ($\Delta S/R$) for the CBS*n*OBO*n*SCB trimers. Upper and bottom lines correspond to heating data (T_m , T_{NI} , $\Delta S_m/R$, and $\Delta S_{NI}/R$) and cooling data (T_{Cr} , T_{NS} , T_{NNTB} , T_{IN} , $\Delta S_{Cr}/R$, and $\Delta S_{IN}/R$), respectively.

<i>n</i>	Cr	T_m (°C)	$\Delta S_m/R$	-	-	N	T_{NI} (°C)	$\Delta S_{NI}/R$	I
		T_{Cr} (°C)	$\Delta S_{Cr}/R$	Monotropic SmA or N _{TB} ^a	T_{NS} or T_{NNTB} (°C)		T_{IN} (°C)	$\Delta S_{IN}/R$	
3	•	186.4	20.9						•
	•	144.8	19.6			•	142 ^a	-	•
4	•	235.3	12.5			•	253.2	2.8	•
	•	196.6	11.9			•	249.5	3.1	•
5	•	171.8	22.5						•
	•	133.6	19.7	N _{TB}	117 ^a	•	154.2	0.4	•
6	•	219.0	24.7						•
	•	200.9	14.9	SmA	180 ^a	•	217.4	4.0	•
7 ^b	•	149.4	20.7			•	162.4	0.8	•
	•	130.0	20.6	N _{TB}	126 ^a	•	160.2	0.7	•
8	•	195.6	31.1 ^d			•	198.8	- ^d	•
	•	168.6	13.2	SmA	167 ^a	•	195.0	4.3	•
9 ^c	•	131.3	21.5			•	158.8	1.1	•
	•	103.6	20.3	N _{TB}	122.7	•	156.5	1.1	•
10	•	184.8	32.8						•
	•	150.7	25.5	SmA	146 ^a	•	176.2	4.9	•
11	•	135.4	29.2			•	154.0	1.7	•
	•	116.6	25.2	N _{TB}	121 ^a	•	151.5	1.7	•

^a Determined by POM. ^b Ref. [62] ^c Ref. [63] ^d Total entropy of ($\Delta S_m/R + \Delta S_{NI}/R$) due to peak overlap.

To analyze the spacer-length dependency of phase-transition behavior, T_{NS} , T_{NNTB} , T_{IN} , and $\Delta S_{IN}/R$ upon cooling are plotted as a function of n for the CBS*n*OBO*n*SCB trimers (Figure 4). Because of the monotropic LC natures for the N (for $n = 3, 5, 6$, and 10) and SmA or N_{TB} phases (for $n = 5$ –11), the cooling data are discussed here. As shown in Figure 4, CBS*n*OBO*n*SCB homologs exhibited clear odd–even oscillations for T_{IN} and $\Delta S_{IN}/R$, with much higher values for even- n than for odd- n . Such oscillation, depending on the parity of n , is also observed for T_m upon heating. These odd–even effects on phase transitions are generally attributed to the different average molecular shapes imposed by spacer parity. Even- n and odd- n make the molecular shapes of LC trimers linear and bent, respectively. It is typically observed that, with increasing n , although the odd–even oscillation magnitude for T_{IN} decreased (or attenuated), the odd–even oscillation for $\Delta S_{IN}/R$ was unattenuated. Interestingly, the T_{NS} and T_{NNTB} of LC trimers visually resembled odd–even oscillations for successive n values, as shown in Figure 4a, despite the different types of LC phases involved. With increasing n , the T_{NS} for even- n decreased sharply, whereas the T_{NNTB} for odd- n slightly increased. Similar trends have been reported for CBO*n*OBO*n*OCB [58]. Even- n homologs formed Sm phases, which are ascribable to their roughly linear shapes and the lengthening of their alkylene spacers that caused a significant separation of parallel oriented biphenyls. The significant decline in T_{NS} with increasing n could be attributed to the C–S–C bond linkage causing high conformational and steric bulkiness of the two rotatable terminal cyanobiphenyls. In contrast, the N_{TB} phase was driven only by bent molecular shapes. The molecular anisotropy of bent LC oligomers, which have an odd number of spacers, increased with the number of spacers. Therefore, the T_{NNTB} increased upon increasing n , and vice versa. The T_{NNTB} values of the biphenyl-based LC trimers (>110 °C) are clearly higher than those of usual biphenyl-based dimers (<100 °C). Increased intermolecular interactions, e.g., higher oligomers [58,76] and extended π -conjugation [70], lead to increasing T_{NNTB} .

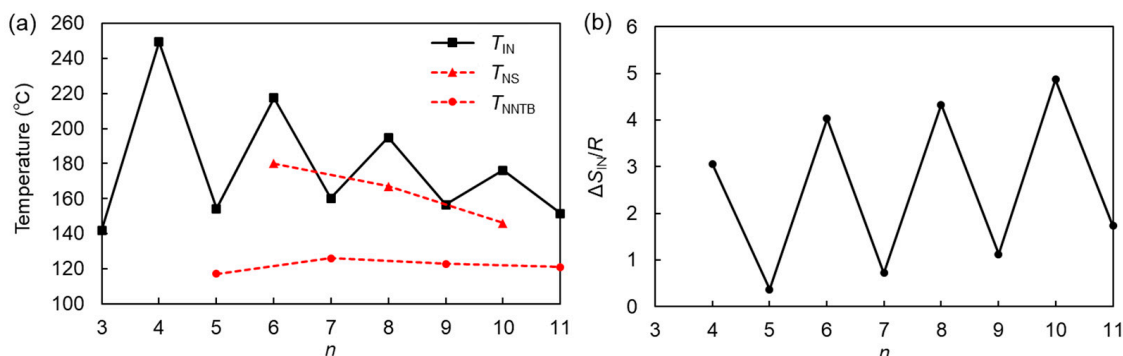


Figure 4. (a) Phase-transition temperatures upon cooling: T_{IN} (squares), T_{NS} (triangles), and T_{NNTB} (circles), and (b) $\Delta S_{IN}/R$ upon cooling, as a function of n , for the CBSnOBOnSCB trimers.

3.2. Comparison of CBSnOBOnSCB and CBO nOBOnOCB

3.2.1. Phase-Transition Behavior

The phase-transition behavior of thioether-linked CBSnOBOnSCB and all-ether-linked CBO nOBOnOCB homologs were compared. T_m , T_{IN} , T_{NS} , T_{NNTB} , N phase temperature range upon cooling (ΔT_N), and $\Delta S_{IN}/R$ of both the homologs are plotted as a function of n (Figure 5). The data for CBO nOBOnOCB is quoted from the literature [58].

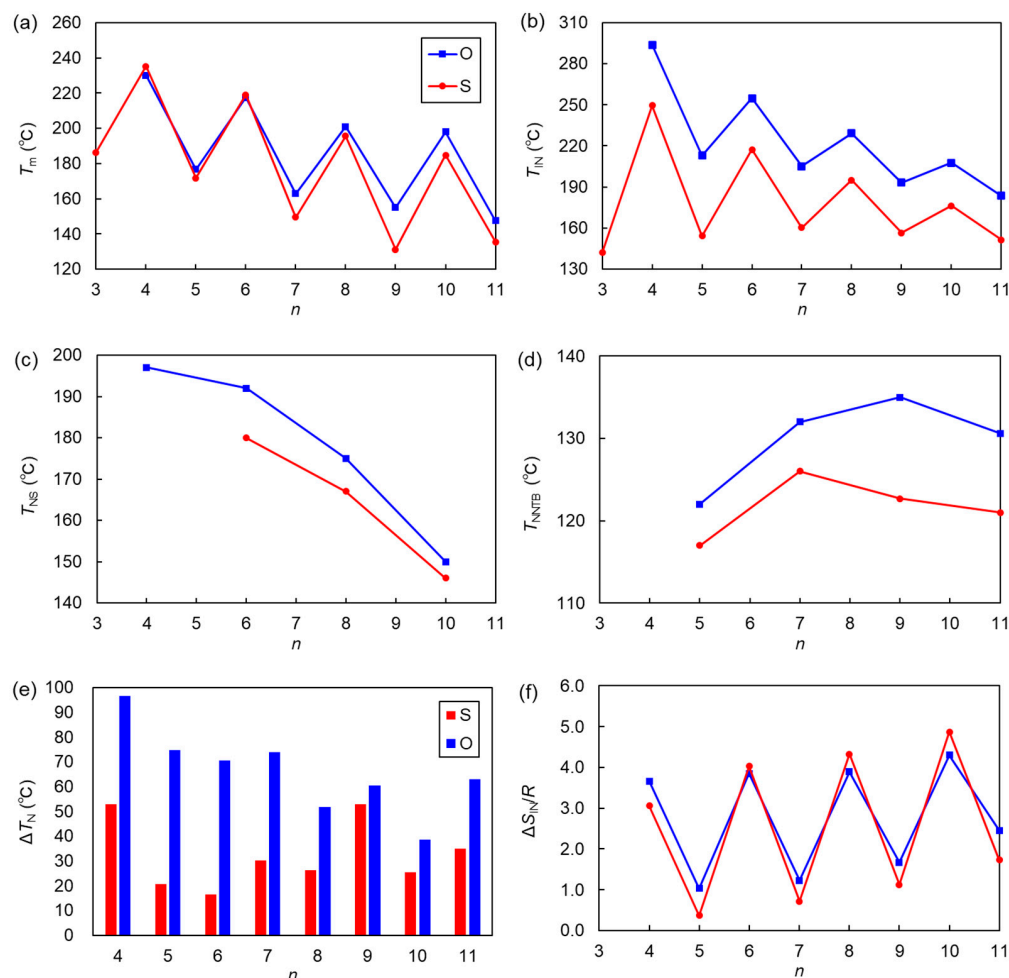


Figure 5. Comparisons of (a) T_m , (b) T_{IN} , (c) T_{NS} , (d) T_{NNTB} , (e) ΔT_N , and (f) $\Delta S_{IN}/R$, as a function of n , for the CBSnOBOnSCB and CBO nOBOnOCB trimer homologs.

As described above, the thioether-linked CBS n OBO n SCB ($n = 4, 7-9$, and 11) exhibited the enantiotropic N phase, whereas the homologs with $n = 3, 5, 6$, and 10 exhibited the monotropic N phase. This differs from the behavior of all-ether-linked CBO n OBO n OCB homologs, which exhibit enantiotropic N phases for all tested n values (4–12) [58–61]. Thus, the replacement of outer ether linkages with thioether reduced the ability of the trimer homologs to form LCs [63], which is similar to the behavior of thioether-containing calamitic LCs [64–67]. This is primarily ascribed to the large conformational flexibility, steric bulkiness, and lower molecular anisotropy (larger molecular width) that the C–S–C bond imparts because it is more flexible, shorter, and has a smaller angle ($\sim 100^\circ$) than the ether C–O–C bond.

Figure 5a shows that the T_m values of both homologs oscillated significantly with the parity of n . The T_m values of thioether-linked CBS n OBO n SCB homologs became lower than those of CBO n OBO n OCB, with increasing n . As shown in Figure 5b–d, the thioether-linked CBS n OBO n SCB homologs exhibited lower T_{IN} , T_{NS} , and T_{NNTB} values than their CBO n OBO n OCB counterparts. Additionally, ΔT_N was smaller (narrower) for thioether-linked CBS n OBO n SCB than for CBO n OBO n OCB, as shown in Figure 5e, primarily because of the lower T_{IN} (or T_{NI}) of CBS n OBO n SCB. In addition to the tendency to form monotropic LCs, the lower phase-transition temperatures and consequent narrower temperature LC phases for thioether-linked LC trimers are primarily ascribed to the greater conformational flexibility, steric bulkiness, and the low molecular anisotropy afforded by flexible C–S–C bonds with smaller inner angles than C–O–C bonds. For bent LC dimers, the thioether linkage causes the LC phases to be significantly supercooled and vitrified. This is a consequence of the synergy between the enhanced bent shape of the entire molecule and the flexibility of the C–S–C bond, which prevents crystallization [68,70–74]. However, such supercooling effects on LC phases were not observed for the thioether-linked trimers in this study, which all crystallized. Notably, Figure 5f reveals that the $\Delta S_{IN}/R$ values of CBS n OBO n SCB were lower and slightly higher than those of CBO n OBO n OCB for odd- n and even- n , respectively. Therefore, the replacement of the outer ether with thioether caused a greater odd–even oscillation in $\Delta S_{IN}/R$. This trend is similar to the difference between methylene- and ether-linked cyanobiphenyl-based dimer homologs (CB n CB and CBO n OCB, respectively), in which the methylene linkages lead to the greater odd–even oscillation than the ether linkages [3]. More specifically, when the spacer has odd- n , $\Delta S_{IN}/R$ is lower for a methylene-linked CB n CB dimer than for an ether-linked CBO n OCB counterpart. This is ascribed to more bent geometry or greater biaxiality for CB n CB, which could be the case for the present trimers that more bent CBS n OBO n SCB show lower $\Delta S_{IN}/R$ than CBO n OBO n OCB. In contrast, when the spacer has even- n , $\Delta S_{IN}/R$ is higher for CB n CB than for CBO n OCB, which is associated with the higher order parameters for CB n CB than for CBO n OCB [3]. This consideration may possibly be linked to the present thioether-linked CBS n OBO n SCB trimers for even- n to be higher $\Delta S_{IN}/R$ than CBO n OBO n OCB.

3.2.2. Mesophase Structures

XRD measurements were performed for thioether-linked CBS9OBO9SCB and all-ether-linked CBO9OBO9OCB, which contain the same nonane spacers. For both these materials, prior crystallization upon cooling, unfortunately, prevented the determination of the diffraction patterns of the monotropic SmA and N_{TB} phases. Therefore, only the data for the upper N phases are described.

Two-dimensional (2D) XRD patterns obtained for the N phases of both trimers showed two symmetric arc-shaped diffractions on the equatorial line in the wide-angle region, as shown in Figures 6a and S13. These indicate the average orientation of the molecular long-axis along the magnetic field directions, denoted by a meridional arrow in Figure 6a. The wide-angle diffractions are associated with average lateral intermolecular correlations. The d -spacing values of the wide-angle diffractions (d_{WAX}) of both trimers were estimated using the Bragg equation and are plotted in Figure 6b as a function of shifted temperature, $\Delta T = T_{IN} - T$, where T refers to measured temperature upon cooling. The d_{WAX} values

were in the range of 4.59–4.66 Å and 4.57–4.73 Å for CBS9OBO9SCB and CBO9OBO9OCB, respectively, and both decreased with a reduction in temperature. As shown in Figure 6b, the d_{WAX} values were slightly smaller for thioether-linked CBS9OBO9SCB compared to the all-ether-linked CBO9OBO9OCB, indicating shorter lateral molecular correlations for the former. This tendency is similar to the behavior of thioether- and ether-containing LCs [65,66,68], and could be caused by two factors. The large dispersion forces provided by the more polarizable sulfur atom likely led to the shorter intermolecular lateral distances, while the electrostatic repulsion of electron-donating-ether-based LCs might lead to longer lateral distances [77].

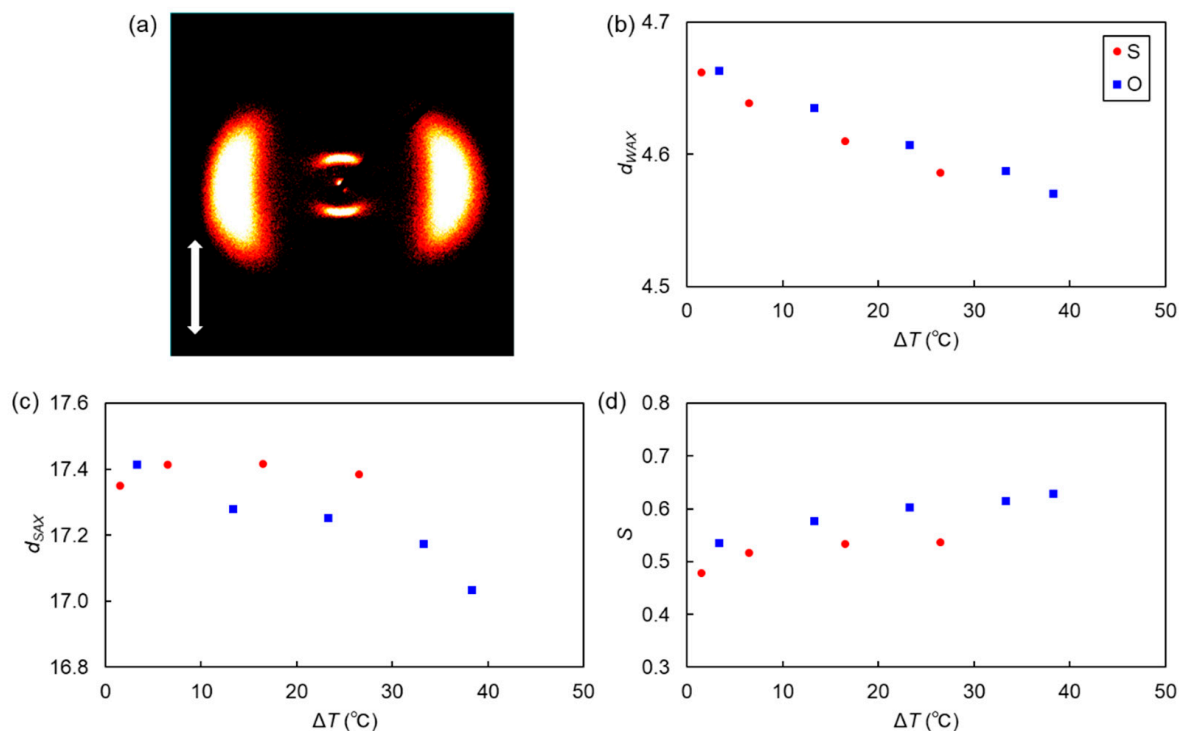


Figure 6. (a) The 2D-XRD pattern of the N phase (155 °C) of CBS9OBO9SCB in a magnetic field denoted by a meridional arrow, and (b) d_{WAX} , (c) d_{SAX} , and (d) S values, as a function of ΔT , for the CBS9OBO9SCB and CBO9OBO9OCB trimer homologs.

Small-angle diffractions, symmetric on the meridional lines (Figures 6a and S13), were observed at $2\theta = \sim 5.1^\circ$ for CBS9OBO9SCB and CBO9OBO9OCB, indicating a strong cybotactic N (N_{Cyb}) tendency with Sm-like clusters [78,79]. Such a pronounced N_{Cyb} trend is ascribable to the strong intermolecular interactions of LC trimers. The small-angle diffractions were not split on the meridional lines, indicating an N_{Cyb} nature consisting of orthogonal SmA-like clusters (namely, an N_{CybA} phase), similar to CBO_nOBO_nOCB ($n = 10, 11$) [58] and fluorenone-based trimer analogs [63]. This could be correlated to SmA phase formation for even- n trimer homologs. The d -spacing values of the small-angle diffractions (d_{SAX}) of CBS9OBO9SCB and CBO9OBO9OCB were ~ 17 Å (Figure 6c), which could be approximately one-third of the average molecular lengths of both trimers. This indicates that this type of LC trimer forms N_{CybA} phases based on triply intercalated structures, irrespective of linkage type (thioether/ether) or spacer parity (even/odd) [58]. Strictly, the d_{SAX} values of all-ether-linked CBO9OBO9OCB seem like becoming gradually smaller than those of thioether-linked CBS9OBO9SCB with increasing ΔT (or decreasing T).

The orientational order parameter (S) values of N phases were evaluated from wide-angle diffractions [6] and are plotted in Figure 6d as a function of ΔT . The S values were approximately 0.4–0.5 for CBS9OBO9SCB and 0.5–0.6 for CBO9OBO9OCB. These values, which are typical for N phases, gradually increased with increasing ΔT (or decreasing

T). Over the entire N phase range, thioether-linked CBS9OBO9SCB exhibited lower S values than CBO9OBO9OCB (Figure 6d). This trend is similar to the difference between *bis*-thioether-linked CBS n SCB and mono-thioether-linked CBS n OCB dimers [68], indicating that replacement of ether with thioether leads to lower apparent S values. It is noted that apparent S values of bent LC dimers and oligomers based on wide-angle diffractions would not simply reflect orientational orders of the global molecular directors with rotational symmetry, which are strongly influenced by molecular biaxiality [3]. The thioether linkage enhances molecular biaxiality (or leads to more bending) due to the small C–S–C bond angle. Therefore, lower estimated apparent S values for thioether-linked dimers and oligomers mirror their more bent geometry in LC states than those of ether-linked analogs.

4. Conclusions

Herein, the development, phase-transition behavior, and mesophase structures of the homologous series of thioether-linked cyanobiphenyl-based trimers possessing a wide range of odd and even numbers of carbon atoms in the alkylene spacers, CBS n OBO n SCB ($n = 3–11$), have been reported for the first time. All CBS n OBO n SCB members exhibited LC phases. Odd–even oscillations in the phase-transition parameters were observed and were typically higher for even- n than for odd- n . Interestingly, even- n and odd- n homologs showed layered SmA and pseudo-layered heliconical N_{TB} phases, respectively. The differences in phase-transition behaviors, depending on the spacer parity of the LC trimers, were attributed to their different average molecular shapes or relative orientations between the biphenyls: A straightened stretched Z-like shape for even- n homologs and an obliquely directed bent shape for the odd- n homologs. Their phase-transition behavior and mesophase structures were compared with those of previously reported all-ether-linked CBO n OBO n OCB homologs. It was revealed that the replacement of outer ether linkages with thioether linkages primarily caused the LC trimers to form monotropic LCs and lower phase-transition temperatures. These phenomena were caused by the enhanced flexibility and bent shape (lower molecular anisotropy) of C–S–C bonds. The XRD analyses revealed that the LC trimers formed a cybotactic N_{CybA} phase with a triply intercalated structure, irrespective of the nature of the linkages (thioethers or ethers) or of spacer parity. This study provides new insights into the influence of thioether (C–S–C) bonds on the phase-transition properties of LC trimers.

Supplementary Materials: The following supporting information can be downloaded at: <https://www.mdpi.com/article/10.3390/ma15051709/s1>, Scheme S1: Synthesis pathway of odd- n CBS n OBO n SCB members; Scheme S2: Synthesis pathway of even- n CBS n OBO n SCB members; Figure S1: POM image of small N domains (140 °C) of CBS3OBO3SCB, developed from its supercooled Iso phase domains in a non-treated glass cell; Figure S2: POM image of a N phase at 140 °C of CBS4OBO4SCB in a non-treated glass cell; Figure S3: POM images of CBS5OBO5SCB, showing (a) a supercooled N domain at 121 °C, (b) a changed texture reminiscent of the N_{TB} phase at 171 °C, and (c) Cr phase at 105 °C in a non-treated glass cell; Figure S4: POM images of CBS8OBO8SCB showing (a) marble and schlieren textures (N phase) at 198 °C and (b) fan-shaped and focal conic textures (SmA phase) at 170 °C in a non-treated glass cell; Figure S5: POM image of fan-shaped and focal conic textures (SmA phase) at 133 °C of CBS10OBO10SCB in a non-treated glass cell; Figure S6: DSC curves of CBS3OBO3SCB; Figure S7: DSC curves of CBS4OBO4SCB; Figure S8: DSC curves of CBS5OBO5SCB; Figure S9: DSC curves of CBS6OBO6SCB; Figure S10: DSC curves of CBS8OBO8SCB; Figure S11: DSC curves of CBS10OBO10SCB; Figure S12: DSC curves of CBS11OBO11SCB; Figure S13: 2D-XRD pattern of the N phase 160 °C of CBO9OBO9OCB in a magnetic field denoted by a meridional arrow.

Author Contributions: Conceptualization, Y.A.; Methodology, Y.A.; Validation, Y.A.; Formal analysis, Y.A., K.K., Y.I., and T.S.; Investigation, Y.A., K.K., Y.I., and T.S.; Resources, Y.A. and H.T.; Data curation, Y.A.; Writing—original draft preparation, Y.A.; Writing—review and editing, Y.A., K.K., Y.I., T.S., and H.T.; Supervision, Y.A. and H.T.; Project administration, Y.A.; Funding acquisition, Y.A. All authors have read and agreed to the published version of the manuscript.

Funding: This research was funded by the Japan Society for the Promotion of Science (KAKENHI grant numbers 17K14493 and 20K15351), the Naito Research Grant, the Toukai Foundation for Technology, and Toyohashi University of Technology.

Institutional Review Board Statement: Not applicable.

Informed Consent Statement: Not applicable.

Data Availability Statement: Data are presented in the article and Supplementary Materials.

Acknowledgments: We would like to thank Masatoshi Tokita for providing us the opportunity for conducting XRD measurements at Tokyo Institute of Technology.

Conflicts of Interest: The authors declare no conflict of interest.

References

1. Imrie, C.T.; Henderson, P.A. Liquid crystal dimers and higher oligomers: Between monomers and polymers. *Chem. Soc. Rev.* **2007**, *36*, 2096–2124. [[CrossRef](#)] [[PubMed](#)]
2. Emsley, J.W.; Luckhurst, G.R.; Shilstone, G.N.; Sage, I. The preparation and properties of the α , ω -bis (4, 4'-cyanobiphenyloxy) alkanes: Nematogenic molecules with a flexible core. *Mol. Cryst. Liq. Cryst.* **1984**, *102*, 223–233. [[CrossRef](#)]
3. Barnes, P.J.; Douglass, A.G.; Heeks, S.K.; Luckhurst, G.R. An enhanced odd-even effect of liquid crystal dimers orientational order in the α , ω -bis (4'-cyanobiphenyl-4-yl) alkanes. *Liq. Cryst.* **1993**, *13*, 603–613. [[CrossRef](#)]
4. Marcelis, A.T.; Koudijs, A.; Sudhölter, E.J. Odd-even effects in the thermotropic and optical properties of three series of chiral twin liquid crystals. *Liq. Cryst.* **1995**, *18*, 843–850. [[CrossRef](#)]
5. Yoshida, T.; Sugimoto, A.; Ikoma, A.; Matsuoka, T.; Kang, S.; Sakajiri, K.; Watanabe, J.; Tokita, M. Odd-even effect on viscoelastic properties of twin-dimer nematic liquid crystals. *Liq. Cryst.* **2015**, *42*, 463–472. [[CrossRef](#)]
6. Arakawa, Y.; Sasaki, S.; Igawa, K.; Tokita, M.; Konishi, G.; Tsuji, H. Birefringence and photoluminescence properties of diphenylacetylene-based liquid crystal dimers. *New J. Chem.* **2020**, *44*, 17531–17541. [[CrossRef](#)]
7. Watanabe, J.; Komura, H.; Niori, T. Thermotropic liquid crystals of polyesters having a mesogenic 4, 4'-bibenzoate unit smectic mesophase properties and structures in dimeric model compounds. *Liq. Cryst.* **1993**, *13*, 455–465. [[CrossRef](#)]
8. Niori, T.; Adachi, S.; Watanabe, J. Smectic mesophase properties of dimeric compounds. 1. Dimeric compounds based on the mesogenic azobenzene unit. *Liq. Cryst.* **1995**, *19*, 139–148. [[CrossRef](#)]
9. Dozov, I. On the spontaneous symmetry breaking in the mesophases of achiral banana-shaped molecules. *Europhys. Lett.* **2001**, *56*, 247–253. [[CrossRef](#)]
10. Memmer, R. Liquid crystal phases of achiral banana-shaped molecules: A computer simulation study. *Liq. Cryst.* **2002**, *29*, 483–496. [[CrossRef](#)]
11. Panov, V.P.; Nagaraj, M.; Vij, J.K.; Panarin, Y.P.; Kohlmeier, A.; Tamba, M.G.; Lewis, R.A.; Mehl, G.H. Spontaneous periodic deformations in nonchiral planar-aligned bimesogens with a nematic-nematic transition and a negative elastic constant. *Phys. Rev. Lett.* **2010**, *105*, 167801. [[CrossRef](#)] [[PubMed](#)]
12. Cestari, M.; Diez-Berart, S.; Dunmur, D.A.; Ferrarini, A.; De La Fuente, M.R.; Jackson, D.J.B.; Lopez, D.O.; Luckhurst, G.R.; Perez-Jubindo, M.A.; Richardson, R.M.; et al. Phase behavior and properties of the liquid-crystal dimer 1'', 7''-bis (4-cyanobiphenyl-4'-yl) heptane: A twist-bend nematic liquid crystal. *Phys. Rev. E* **2011**, *84*, 031704. [[CrossRef](#)] [[PubMed](#)]
13. Chen, D.; Porada, J.H.; Hooper, J.B.; Klittnick, A.; Shen, Y.; Tuchband, M.R.; Korblova, E.; Bedrov, D.; Walba, D.M.; Glaser, M.A.; et al. Chiral heliconical ground state of nanoscale pitch in a nematic liquid crystal of achiral molecular dimers. *Proc. Natl. Acad. Sci. USA* **2013**, *110*, 15931–15936. [[CrossRef](#)] [[PubMed](#)]
14. Borshch, V.; Kim, Y.K.; Xiang, J.; Gao, M.; Jáklí, A.; Panov, V.P.; Vij, J.K.; Imrie, C.T.; Tamba, M.G.; Mehl, G.H.; et al. Nematic twist-bend phase with nanoscale modulation of molecular orientation. *Nat. Commun.* **2013**, *4*, 2635. [[CrossRef](#)]
15. Zhu, C.; Tuchband, M.R.; Young, A.; Shuai, M.; Scarbrough, A.; Walba, D.M.; Maclennan, J.E.; Wang, C.; Hexemer, A.; Clark, N.A. Resonant carbon K-edge soft X-ray scattering from lattice-free heliconical molecular ordering: Soft dilative elasticity of the twist-bend liquid crystal phase. *Phys. Rev. Lett.* **2016**, *116*, 147803. [[CrossRef](#)] [[PubMed](#)]
16. Salili, S.M.; Kim, C.; Sprunt, S.; Gleeson, J.T.; Parri, O.; Jáklí, A. Flow properties of a twist-bend nematic liquid crystal. *RSC Adv.* **2014**, *4*, 57419–57423. [[CrossRef](#)]
17. Challa, P.K.; Borshch, V.; Parri, O.; Imrie, C.T.; Sprunt, S.N.; Gleeson, J.T.; Lavrentovich, O.D.; Jáklí, A. Twist-bend nematic liquid crystals in high magnetic fields. *Phys. Rev. E* **2014**, *89*, 060501. [[CrossRef](#)]
18. Gorecka, E.; Vaupotič, N.; Zep, A.; Pocięcha, D.; Yoshioka, J.; Yamamoto, J.; Takezoe, H. A Twist-Bend Nematic (N_{TB}) Phase of Chiral Materials. *Angew. Chem. Int. Ed.* **2015**, *54*, 10155–10159. [[CrossRef](#)]
19. Zhou, J.; Tang, W.; Arakawa, Y.; Tsuji, H.; Aya, S. Viscoelastic properties of a thioether-based heliconical twist-bend nematic. *Phys. Chem. Chem. Phys.* **2020**, *22*, 9593–9599. [[CrossRef](#)]
20. Kumar, M.P.; Kula, P.; Dhara, S. Smecticlike rheology and pseudolayer compression elastic constant of a twist-bend nematic liquid crystal. *Phys. Rev. Mater.* **2020**, *4*, 115601. [[CrossRef](#)]

21. Meyer, C.; Luckhurst, G.R.; Dozov, I. The temperature dependence of the heliconical tilt angle in the twist-bend nematic phase of the odd dimer CB7CB. *J. Mater. Chem. C* **2015**, *3*, 318–328. [[CrossRef](#)]
22. Sebastián, N.; López, D.O.; Robles-Hernández, B.; de la Fuente, M.R.; Salud, J.; Pérez-Jubindo, M.A.; Dunmur, D.A.; Luckhurst, G.R.; Jackson, D.J.B. Dielectric, calorimetric and mesophase properties of 1''-(2', 4-difluorobiphenyl-4'-yloxy)-9''-(4-cyanobiphenyl-4'-yloxy) nonane: An odd liquid crystal dimer with a monotropic mesophase having the characteristics of a twist-bend nematic phase. *Phys. Chem. Chem. Phys.* **2014**, *16*, 21391–21406. [[CrossRef](#)] [[PubMed](#)]
23. Paterson, D.A.; Xiang, J.; Singh, G.; Walker, R.; Agra-Kooijman, D.M.; Martínez-Felipe, A.; Gao, M.; Storey, J.M.D.; Kumar, S.; Lavrentovich, O.D.; et al. Reversible isothermal twist–bend nematic–nematic phase transition driven by the photoisomerization of an azobenzene-based nonsymmetric liquid crystal dimer. *J. Am. Chem. Soc.* **2016**, *138*, 5283–5289. [[CrossRef](#)] [[PubMed](#)]
24. Panov, V.P.; Sreenilayam, S.P.; Panarin, Y.P.; Vij, J.K.; Welch, C.J.; Mehl, G.H. Characterization of the submicrometer hierarchy levels in the twist-bend nematic phase with nanometric helices via photopolymerization. Explanation for the sign reversal in the polar response. *Nano Lett.* **2017**, *17*, 7515–7519. [[CrossRef](#)]
25. Prasad, S.K.; Madhuri, P.L.; Satapathy, P.; Yelamagad, C.V. A soft-bent dimer composite exhibiting twist-bend nematic phase: Photo-driven effects and an optical memory device. *Appl. Phys. Lett.* **2018**, *112*, 253701. [[CrossRef](#)]
26. Merkel, K.; Kocot, A.; Vij, J.K.; Shanker, G. Distortions in structures of the twist bend nematic phase of a bent-core liquid crystal by the electric field. *Phys. Rev. E* **2018**, *98*, 022704. [[CrossRef](#)]
27. Aya, S.; Salamon, P.; Paterson, D.A.; Storey, J.M.; Imrie, C.T.; Araoka, F.; Jákli, A.; Buka, Á. Fast-and-giant photorheological effect in a liquid crystal dimer. *Adv. Mater. Interfaces* **2019**, *6*, 1802032. [[CrossRef](#)]
28. Feng, C.; Feng, J.; Saha, R.; Arakawa, Y.; Gleeson, J.; Sprunt, S.; Zhu, C.; Jákli, A. Manipulation of the nanoscale heliconical structure of a twist-bend nematic material with polarized light. *Phys. Rev. Res.* **2020**, *2*, 032004. [[CrossRef](#)]
29. Stevenson, W.D.; Zeng, X.; Welch, C.; Thakur, A.K.; Ungar, G.; Mehl, G.H. Macroscopic chirality of twist-bend nematic phase in bent dimers confirmed by circular dichroism. *J. Mater. Chem. C* **2020**, *8*, 1041–1047. [[CrossRef](#)]
30. Merkel, K.; Loska, B.; Welch, C.; Mehl, G.H.; Kocot, A. Molecular biaxiality determines the helical structure–infrared measurements of the molecular order in the nematic twist-bend phase of difluoro terphenyl dimer. *Phys. Chem. Chem. Phys.* **2021**, *23*, 4151–4160. [[CrossRef](#)]
31. Cao, Y.; Feng, J.; Nallapaneni, A.; Arakawa, Y.; Zhao, K.; Zhang, H.; Mehl, G.H.; Zhu, C.; Liu, F. Deciphering helix assembly in the heliconical nematic phase via tender resonant X-ray scattering. *J. Mater. Chem. C* **2021**, *9*, 10020–10028. [[CrossRef](#)]
32. Varshini, G.V.; Rao, D.S.; Hiremath, U.S.; Yelamagad, C.V.; Prasad, S.K. Dielectric and viscoelastic investigations in a binary system of soft-and rigid-bent mesogens exhibiting the twist-bend nematic phase. *J. Mol. Liq.* **2021**, *323*, 114987. [[CrossRef](#)]
33. Vanakaras, A.G.; Photinos, D.J. A molecular theory of nematic–nematic phase transitions in mesogenic dimers. *Soft Matter* **2016**, *12*, 2208–2220. [[CrossRef](#)] [[PubMed](#)]
34. Heist, L.M.; Samulski, E.T.; Welch, C.; Ahmed, Z.; Mehl, G.H.; Vanakaras, A.G.; Photinos, D.J. Probing molecular ordering in the nematic phases of para-linked bimesogen dimers through NMR studies of flexible prochiral solutes. *Liq. Cryst.* **2020**, *47*, 2058–2073. [[CrossRef](#)]
35. Samulski, E.T.; Reyes-Arango, D.; Vanakaras, A.G.; Photinos, D.J. All Structures Great and Small: Nanoscale Modulations in Nematic Liquid Crystals. *Nanomaterials* **2022**, *12*, 93. [[CrossRef](#)]
36. Henderson, P.A.; Imrie, C. T Methylene-linked liquid crystal dimers and the twist-bend nematic phase. *Liq. Cryst.* **2011**, *38*, 1407–1414. [[CrossRef](#)]
37. Zep, A.; Aya, S.; Aihara, K.; Ema, K.; Pocięcha, D.; Madrak, K.; Bernatowicz, P.; Takezoe, H.; Gorecka, E. Multiple nematic phases observed in chiral mesogenic dimers. *J. Mater. Chem. C* **2013**, *1*, 46–49. [[CrossRef](#)]
38. Ahmed, Z.; Welch, C.; Mehl, G.H. The design and investigation of the self-assembly of dimers with two nematic phases. *RSC Adv.* **2015**, *5*, 93513–93521. [[CrossRef](#)]
39. Tamba, M.G.; Salili, S.M.; Zhang, C.; Jákli, A.; Mehl, G.H.; Stannarius, R.; Eremin, A. A fibre forming smectic twist–bend liquid crystalline phase. *RSC Adv.* **2015**, *5*, 11207–11211. [[CrossRef](#)]
40. Mandle, R.J.; Goodby, J.W. Does Topology Dictate the Incidence of the Twist-Bend Phase? Insights Gained from Novel Unsymmetrical Bimesogens. *Chem. Eur. J.* **2016**, *22*, 18456–18464. [[CrossRef](#)]
41. Dawood, A.A.; Gossel, M.C.; Luckhurst, G.R.; Richardson, R.M.; Timimi, B.A.; Wells, N.J.; Yousif, Y.Z. On the twist-bend nematic phase formed directly from the isotropic phase. *Liq. Cryst.* **2016**, *43*, 2–12. [[CrossRef](#)]
42. Mandle, R.J.; Archbold, C.T.; Sarju, J.P.; Andrews, J.L.; Goodby, J.W. The dependency of nematic and twist-bend mesophase formation on bend angle. *Sci. Rep.* **2016**, *6*, 36682. [[CrossRef](#)] [[PubMed](#)]
43. Ivšić, T.; Baumeister, U.; Dokli, I.; Mikleušević, A.; Lesac, A. Sensitivity of the N_{TB} phase formation to the molecular structure of imino-linked dimers. *Liq. Cryst.* **2017**, *44*, 93–105.
44. Knežević, A.; Sapunar, M.; Buljan, A.; Dokli, I.; Hameršak, Z.; Kontrec, D.; Lesac, A. Fine-tuning the effect of π – π interactions on the stability of the N_{TB} phase. *Soft Matter* **2018**, *14*, 8466–8474. [[CrossRef](#)]
45. Watanabe, K.; Tamura, T.; Kang, S.; Tokita, M. Twist bend nematic liquid crystals prepared by one-step condensation of 4-(4-Pentylcyclohexyl) benzoic acid and alkyl diol. *Liq. Cryst.* **2018**, *45*, 924–930. [[CrossRef](#)]
46. Walker, R.; Pocięcha, D.; Storey, J.M.D.; Gorecka, E.; Imrie, C.T. The chiral twist-bend nematic phase (N^*_{TB}). *Chem. Eur. J.* **2019**, *25*, 13329–13335. [[CrossRef](#)]

47. Mandle, R.J.; Goodby, J.W. Molecular Flexibility and Bend in Semi-Rigid Liquid Crystals: Implications for the Heliconical Nematic Ground State. *Chem. Eur. J.* **2019**, *25*, 14454–14459. [[CrossRef](#)]
48. Zep, A.; Pruszkowska, K.; Dobrzycki, Ł.; Sektas, K.; Szałański, P.; Marek, P.H.; Cyrański, M.K.; Siciński, R.R. Cholesterol-based photo-switchable mesogenic dimers. Strongly bent molecules versus an intercalated structure. *CrystEngComm* **2019**, *21*, 2779–2789. [[CrossRef](#)]
49. Knežević, A.; Dokli, I.; Novak, J.; Kontrec, D.; Lesac, A. Fluorinated twist-bend nematogens: The role of intermolecular interaction. *Liq. Cryst.* **2021**, *48*, 756–766. [[CrossRef](#)]
50. Wang, Y.; Singh, G.; Agra-Kooijman, D.M.; Gao, M.; Bisoyi, H.K.; Xue, C.; Fisch, M.R.; Kumar, S.; Li, Q. Room temperature heliconical twist-bend nematic liquid crystal. *CrystEngComm* **2015**, *17*, 2778–2782. [[CrossRef](#)]
51. Jansze, S.M.; Martínez-Felipe, A.; Storey, J.M.; Marcelis, A.T.; Imrie, C.T. A twist-bend nematic phase driven by hydrogen bonding. *Angew. Chem.* **2015**, *127*, 653–656. [[CrossRef](#)]
52. Mandle, R.J.; Goodby, J.W. A Liquid Crystalline Oligomer Exhibiting Nematic and Twist-Bend Nematic Mesophases. *ChemPhysChem* **2016**, *17*, 967–970. [[CrossRef](#)] [[PubMed](#)]
53. Mandle, R.J.; Goodby, J.W. Progression from nano to macro science in soft matter systems: Dimers to trimers and oligomers in twist-bend liquid crystals. *RSC Adv.* **2016**, *6*, 34885–34893. [[CrossRef](#)]
54. Saha, R.; Babakhanova, G.; Parsouzi, Z.; Rajabi, M.; Gyawali, P.; Welch, C.; Mehl, G.H.; Gleeson, J.; Lavrentovich, O.D.; Sprunt, S.; et al. Oligomeric odd–even effect in liquid crystals. *Mater. Horiz.* **2019**, *6*, 1905–1912. [[CrossRef](#)]
55. Stevenson, W.D.; An, J.; Zeng, X.B.; Xue, M.; Zou, H.X.; Liu, Y.S.; Ungar, G. Twist-bend nematic phase in biphenylethane-based copolyethers. *Soft Matter* **2018**, *14*, 3003–3011. [[CrossRef](#)]
56. Chen, D.; Nakata, M.; Shao, R.; Tuchband, M.R.; Shuai, M.; Baumeister, U.; Weissflog, W.; Walba, D.M.; Glaser, M.A.; MacLennan, J.E.; et al. Twist-bend heliconical chiral nematic liquid crystal phase of an achiral rigid bent-core mesogen. *Phys. Rev. E* **2014**, *89*, 022506. [[CrossRef](#)]
57. Sreenilayam, S.P.; Panov, V.P.; Vij, J.K.; Shanker, G. The N_{TB} phase in an achiral asymmetrical bent-core liquid crystal terminated with symmetric alkyl chains. *Liq. Cryst.* **2017**, *44*, 244–253. [[CrossRef](#)]
58. Arakawa, Y.; Komatsu, K.; Shiba, T.; Tsuji, H. Phase behaviors of classic liquid crystal dimers and trimers: Alternate induction of smectic and twist-bend nematic phases depending on spacer parity for liquid crystal trimers. *J. Mol. Liq.* **2021**, *326*, 115319. [[CrossRef](#)]
59. Furuya, H.; Asahi, K.; Abe, A. An odd–even effect in the mesophasic behavior of dimer liquid crystals due to the bond orientation of a phenylene unit incorporated in the flexible spacer. *Polym. J.* **1986**, *18*, 779–782. [[CrossRef](#)]
60. Zuev, V.V. Synthesis of Bis (4-cyanobiphenyloxyalkyloxy)-4, 4'-biphenyls, the Liquid-Crystalline Trimers. *Russ. J. Gen. Chem.* **1997**, *67*, 1791–1793.
61. Imrie, C.T.; Luckhurst, G.R. Liquid crystal trimers. The synthesis and characterisation of the 4, 4'-bis [ω -(4-cyanobiphenyl-4'-yloxy) alkoxy] biphenyls. *J. Mater. Chem.* **1998**, *8*, 1339–1343. [[CrossRef](#)]
62. Arakawa, Y.; Komatsu, K.; Inui, S.; Tsuji, H. Thioether-linked liquid crystal dimers and trimers: The twist-bend nematic phase. *J. Mol. Struct.* **2020**, *1199*, 126913. [[CrossRef](#)]
63. Arakawa, Y.; Komatsu, K.; Tsuji, H. 2,7-substituted fluorenone-based liquid crystal trimers: Twist-bend nematic phase induced by outer thioether linkage. 2022. [[CrossRef](#)]
64. Kleinpeter, E.; Köhler, H.; Lunow, A.; Tschierske, C.; Zschke, H. Liquid-crystalline behaviour of 2, 5-disubstituted 1, 3-dioxanes subject to the flexibility of terminal chains. *Tetrahedron* **1988**, *44*, 1609–1612. [[CrossRef](#)]
65. Arakawa, Y.; Kang, S.; Tsuji, H.; Watanabe, J.; Konishi, G. Development of novel bistolane-based liquid crystalline molecules with an alkylsulfanyl group for highly birefringent materials. *RSC Adv.* **2016**, *6*, 16568–16574. [[CrossRef](#)]
66. Arakawa, Y.; Sasaki, Y.; Igawa, K.; Tsuji, H. Hydrogen bonding liquid crystalline benzoic acids with alkylthio groups: Phase transition behavior and insights into the cybotactic nematic phase. *New J. Chem.* **2017**, *41*, 6514–6522. [[CrossRef](#)]
67. Arakawa, Y.; Tsuji, H. Phase transitions and birefringence of bistolane-based nematic molecules with an alkyl, alkoxy and alkylthio group. *Mol. Cryst. Liq. Cryst.* **2017**, *647*, 422–429. [[CrossRef](#)]
68. Arakawa, Y.; Komatsu, K.; Tsuji, H. Twist-bend nematic liquid crystals based on thioether linkage. *New J. Chem.* **2019**, *43*, 6786–6793. [[CrossRef](#)]
69. Cruickshank, E.; Salamończyk, M.; Pocięcha, D.; Strachan, G.J.; Storey, J.M.; Wang, C.; Feng, J.; Zhu, C.; Gorecka, E.; Imrie, C.T. Sulfur-linked cyanobiphenyl-based liquid crystal dimers and the twist-bend nematic phase. *Liq. Cryst.* **2019**, *46*, 1595–1609. [[CrossRef](#)]
70. Arakawa, Y.; Ishida, Y.; Tsuji, H. Ether-and Thioether-Linked Naphthalene-Based Liquid-Crystal Dimers: Influence of Chalcogen Linkage and Mesogenic-Arm Symmetry on the Incidence and Stability of the Twist–Bend Nematic Phase. *Chem. Eur. J.* **2020**, *26*, 3767–3775. [[CrossRef](#)]
71. Arakawa, Y.; Komatsu, K.; Feng, J.; Zhu, C.; Tsuji, H. Distinct twist-bend nematic phase behaviors associated with the ester-linkage direction of thioether-linked liquid crystal dimers. *Mater. Adv.* **2021**, *2*, 261–272. [[CrossRef](#)]
72. Arakawa, Y.; Komatsu, K.; Shiba, T.; Tsuji, H. Methylene-and thioether-linked cyanobiphenyl-based liquid crystal dimers CB n SCB exhibiting room temperature twist-bend nematic phases and glasses. *Mater. Adv.* **2021**, *2*, 1760–1773. [[CrossRef](#)]
73. Arakawa, Y.; Komatsu, K.; Ishida, Y.; Igawa, K.; Tsuji, H. Carbonyl-and thioether-linked cyanobiphenyl-based liquid crystal dimers exhibiting twist-bend nematic phases. *Tetrahedron* **2021**, *81*, 131870. [[CrossRef](#)]

74. Arakawa, Y.; Ishida, Y.; Komatsu, K.; Arai, Y.; Tsuji, H. Thioether-linked benzylideneaniline-based twist-bend nematic liquid crystal dimers: Insights into spacer lengths, mesogenic arm structures, and linkage types. *Tetrahedron* **2021**, *95*, 132351. [[CrossRef](#)]
75. Arakawa, Y.; Tsuji, H. Selenium-linked liquid crystal dimers for twist-bend nematogens. *J. Mol. Liq.* **2019**, *289*, 111097. [[CrossRef](#)]
76. Mandle, R.J.; Goodby, J.W. A Nanohelicoidal Nematic Liquid Crystal Formed by a Non-Linear Duplexed Hexamer. *Angew. Chem. Int. Ed.* **2018**, *57*, 7096–7100. [[CrossRef](#)]
77. Arakawa, Y.; Inui, S.; Tsuji, H. Synthesis and characterization of alkylthio-attached azobenzene-based liquid crystal polymers: Roles of the alkylthio bond and polymer chain in phase behavior and liquid crystal formation. *Polymer* **2021**, *233*, 124194. [[CrossRef](#)]
78. Vries, A.D. X-ray photographic studies of liquid crystals I. A cybotactic nematic phase. *Mol. Cryst. Liq. Cryst.* **1970**, *10*, 219–236. [[CrossRef](#)]
79. Tschierske, C.; Photinos, D.J. Biaxial nematic phases. *J. Mater. Chem.* **2010**, *20*, 4263–4294. [[CrossRef](#)]